Performance design of hypervelocity shock tube facilities

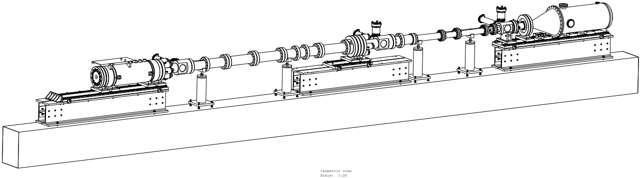

Diana Luís

Instituto Superior Técnico

September 25, 2018

Outline

Outline

Context

- 50 years of planetary landings
- Mission to asteroids, comets and planetary sample return imply high speed Earth reentries (up to 13 km/s)
- US National Research Council "Vision and Voyages for Planetary Science in the Decade 2013-2022" identified probes to Uranus and Saturn as high priorities
- Europe priority is Mars exploration and also renewed interest in Gas Giants

Figure 1: Artists rendition of the Galileo Probe's entry into Jupiter [1]

Outline

World outlook

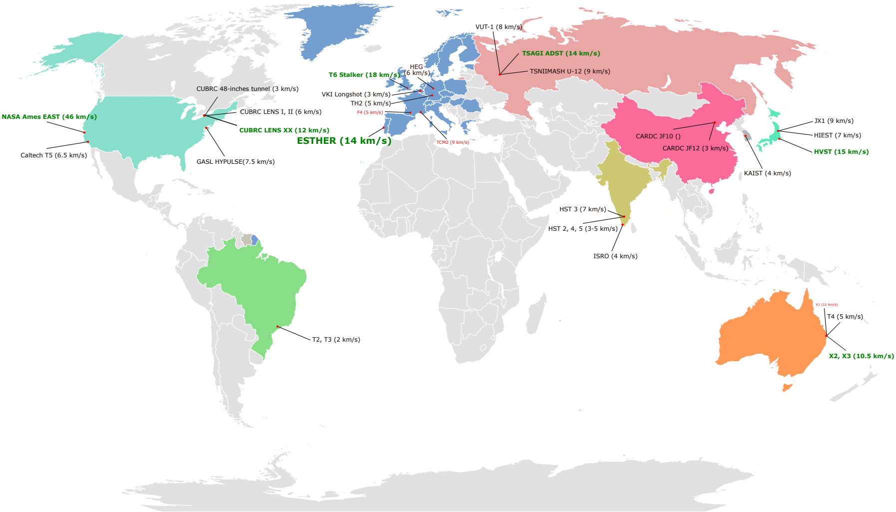

Figure 2: World outlook of hypersonic facilities.

ESTHER shock tube

- New kinetic shock tube being developed by international consortium led by IST.
- Support planetary exploration missions, by studying high-speed radiative and chemical processes kinetics relevant to planetary entries

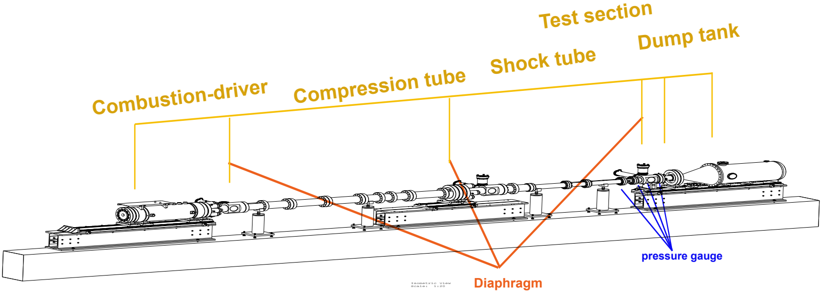

Figure 3: Schematic view of ESTHER shock tube.

Outline

Ideal shock tube theory

- The simplest shock tube consists of two sections separated by a single diaphragm

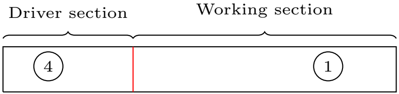

Ideal shock tube theory

- The simplest shock tube consists of two sections separated by a single diaphragm

- The gas expands towards the working section, causing a normal shock wave

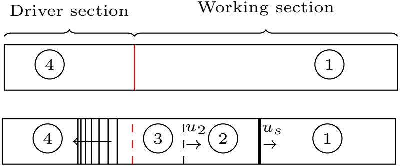

Figure 4: Flow diaphragm of a constant area ratio shock tube [not at scale].

- The shock wave propagates to the left with velocity u_s, increasing the pressure behind it (region 2) and induces a mass motion with velocity u_2
- Simultaneously, the expansion waves move into the high pressure section

$$\frac{p_4}{p_1} = \frac{p_2}{p_1}\left\{1 - \frac{(\gamma_4 - 1)\left(\frac{a_1}{a_4}\right)\left(\frac{p_2}{p_1} - 1\right)}{\sqrt{2\gamma_1\left[2\gamma_1 + (\gamma_1 + 1)\left(\frac{p_2}{p_1} - 1\right)\right]}}\right\}^{-\frac{2\gamma_4}{\gamma_4 - 1}} \tag{1}$$

Design enhancement

A simple shock tube cannot generate shock with extremely high Mach numbers and, in consequence, the gas temperature attainable in such a tube is low.

A simple shock tube cannot generate shock with extremely high Mach numbers and, in consequence, the gas temperature attainable in such a tube is low.

Single diaphragm with variable area shock tube

- Cross-section area reduction at the diaphragm is equivalent to an increase of the driver gas temperature

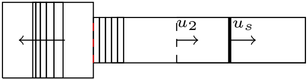

Figure 5: Flow diagram of shock tube with convergent geometry [not at scale].

A simple shock tube cannot generate shock with extremely high Mach numbers and, in consequence, the gas temperature attainable in such a tube is low.

Single diaphragm with variable area shock tube

- Cross-section area reduction at the diaphragm is equivalent to an increase of the driver gas temperature

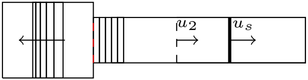

Figure 5: Flow diagram of shock tube with convergent geometry [not at scale].

Double diaphragm shock tube

- An intermediate section allows the main shock wave to be produced from a primary shock wave, reaching higher velocities

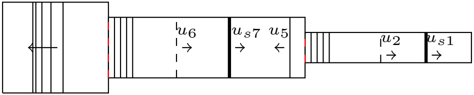

Figure 6: Flow diagram of a double shock tube with cross-section area reductions [not to scale].

Disturbance effects

Wall boundary layer and wall drag effects

- The presence of a wall boundary layer removes mass from region 2, causing the shock to decelerate and the contact surface to accelerate, decreasing the effective test time
- Milne [2] developed a theory to estimate the effects of the shock-boundary layer interaction by adding a source term to the ideal case

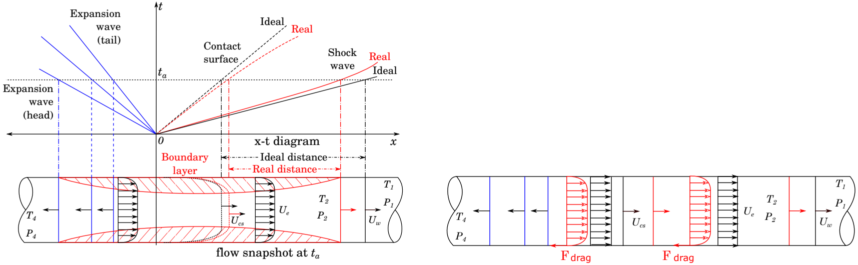

(a) Boundary layer development [not to scale].

(b) Wall drag effects [not to scale].

Figure 7: Disturbance effects.

Blast wave formation

- For sufficiently long working sections, the wave structure evolves into a shape resembling an air blast wave

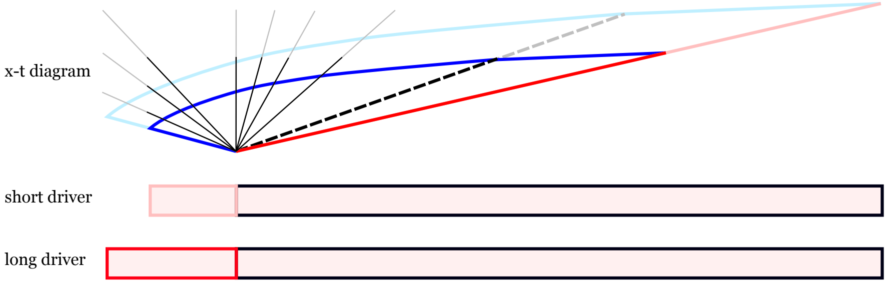

Figure 8: Blast wave formation [not to scale].

Outline

Table 1: Initial properties considered.

	Section	
	Driver	Intermediate
Temperature (in K)	2800	300
Specific heats ratio	1.56	1.667
Molar mass (in g/mol)	7.1	4.0
Gas composition	7:2:1 He:H_2:O_2	Ideal

Test gases

- Earth: 78% N_2, 21% O_2 and 1% Ar
- Mars (and Venus): 95.7% CO_2, 2.7% N_2 and 1.6% Ar
- Titan: 98.5% N_2 and 1.55% CH_4
- Gas Giants: 90% H_2 and 10% He

Area ratio gains

$$u_s = f\left(\frac{A_{11}}{A_1}\right)$$

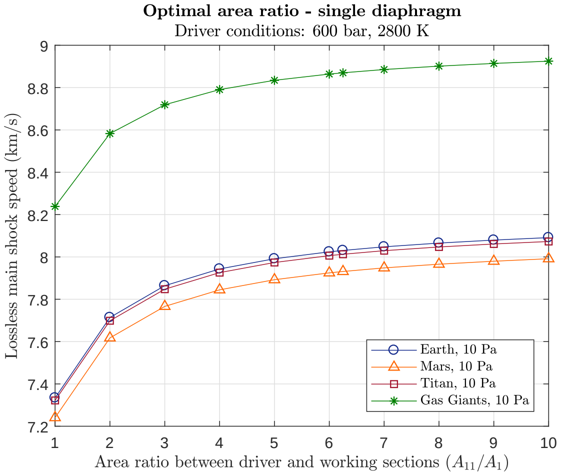

Figure 9: Effect of area ratio on shock speed.

Area ratio gains

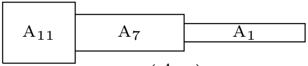

$$u_s = f\left(\frac{A_{11}}{A_1}\right)$$

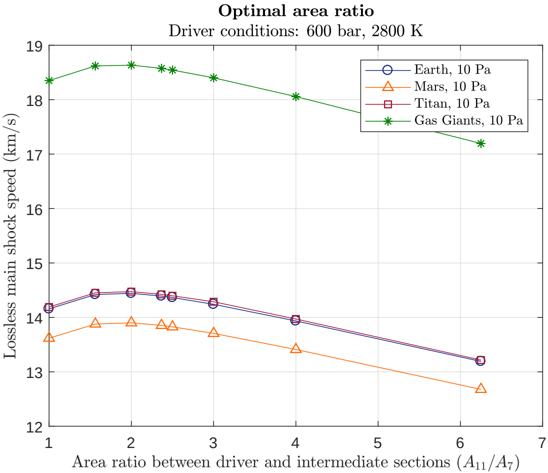

Figure 10: Effect of area ratio on shock speed.

Intermediate pressure optimization

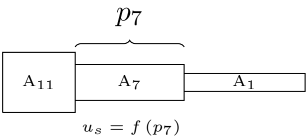

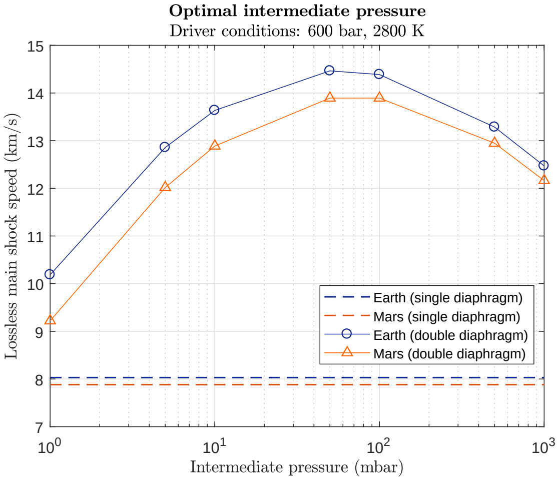

Figure 11: Effect of intermediate pressure.

TÉCNICO LISBOA

ESTHER envelope performance

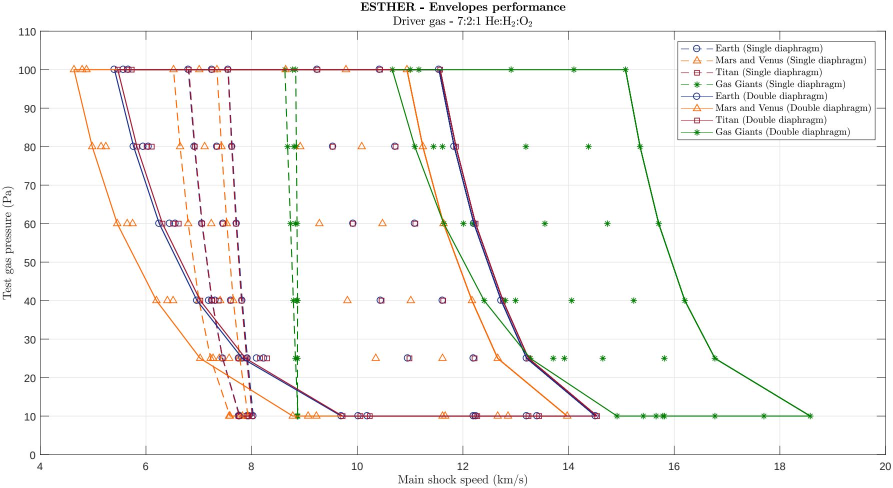

Figure 12: ESTHER shock tube envelope performance for different planetary atmospheres.

Double diaphragm configuration

- Conditions for driver, intermediate and working sections:
  - Minimum speed: 100 bar, 100 Pa and 100 Pa
  - Maximum speed: 600 bar, optimal and 10 Pa

Table 2: Extreme speeds expected.

Atmosphere	Minimum shock speed (km/s)	Maximum shock speed (km/s)
Earth (78% N_2, 21% O_2, 1% Ar)	5.37	14.44
Mars and Venus (95.7% CO_2, 2.7% N_2, 1.6% Ar)	4.60	13.85
Titan (98.5% N_2, 1.5% CH_4)	5.44	14.50
Gas Giants (90% H_2, 10% He)	10.61	18.36

Gas substitutions

- Stalker and Edward [3] proposed increasing the molar percentage of helium above the true atmospheric composition, or substituting it with neon

Gas substitutions

- Stalker and Edward [3] proposed increasing the molar percentage of helium above the true atmospheric composition, or substituting it with neon

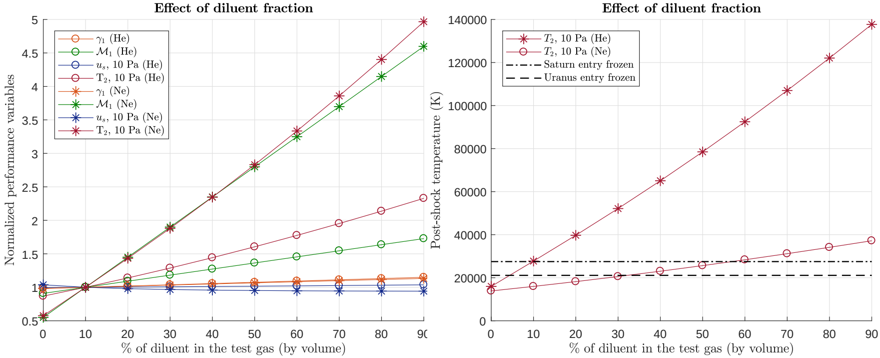

(a) Normalized performance variables.

(b) Post-shock temperature.

Figure 13: Effects of helium and neon diluent.

Test times

- Test times between 3 μs and 30 μs
- Worst estimated test times correspond to Gas Giants' atmosphere

Test times

- Test times between 3 μs and 30 μs
- Worst estimated test times correspond to Gas Giants' atmosphere

Wall loss velocities

- Independent of the shock tube configuration, driver pressure and test gas
- Wall losses between 30 m/s and 50 m/s
- Exception observed for Gas Giants with wall losses between 57 m/s and 200 m/s

Blast wave formation

- Blast wave predicted to form almost 800 m and 150 m after the first diaphragm (single and double diaphragm configurations)
- Confirmed by the characteristic method implemented

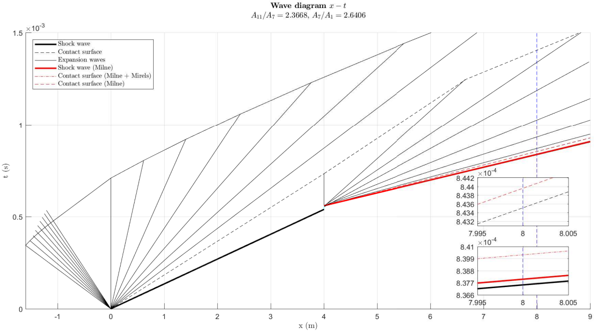

Figure 14: Wave diaphragm for ESTHER in double diaphragm configuration.

Outline

Heaviside signal

- Input signal: heaviside signals
- Output signal: response to a Butterworth second order filter

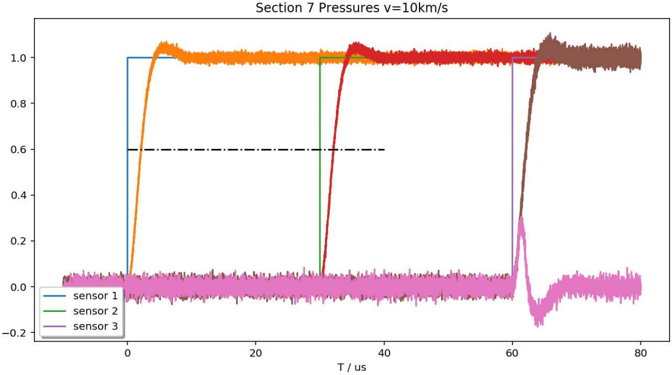

Figure 15: Simulation with a heaviside signal.

Trigger generation

Representative signal

- To more accurately study and predict the behaviour of the trigger system, a representative signal from the X2 expansion tube was extracted from James et al. [4]

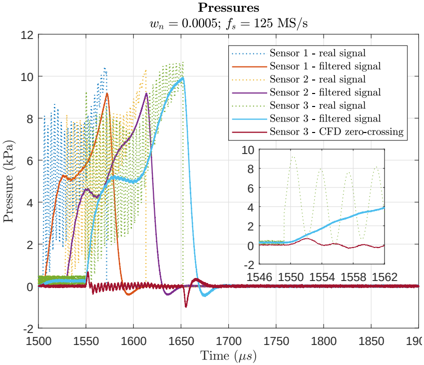

(a) $\omega_n = 0.0005$

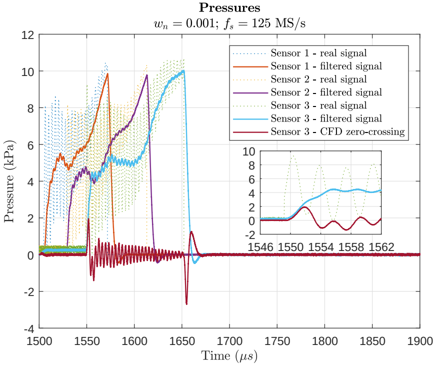

(b) $\omega_n = 0.001$

Figure 16: Filtered signal pressures.

Outline

Achievements

- Performance optimization:
  - High speed: areas and intermediate pressure
  - Low speed: intermediate pressure
- ESTHER compliant for:
  - Earth, Venus, Titan high speed entries
  - Mars high and low speed entries
  - Gas Giants with H_2/He or H_2/Ne substitutions
- Non ideal effects:
  - Mirels' theory: very small test times ($10^{-6} - 10^{-5}$s)
  - Milne drag effects negligible (< 50 m/s, except for Gas Giant < 200 m/s)
  - No risk of blast wave formation (two theories cross-checked)
- Improved trigger system design, accurate up to 18 km/s

- National Aeronautics and Space Administration. https://apod.nasa.gov/apod/ap951208.html, Accessed on September 23, 2018.
- A. Milne, "Wall effects in a 1D shock tube." Private communication, July 2017.
- R. J. Stalker and B. P. Edwards, "Hypersonic blunt-body flowns in hydrogen-neon mixtures," *Journal of Spacecraft and Rockets*, vol. 35, no. 6, pp. 729–735. http://doi.org/10.2514/2.3399.
- C. M. James, D. E. Gildfind, S. Lewis, R. G. Morgan, and F. Zander, "Implementation of a state-to-state analytical framework for the calculation of expansion tube flow properties," *Shock Waves*, vol. 28, pp. 349–377, 2018. http://doi.org/10.1007/s00193-017-0763-3.